Abdominal Radiology (2021) 46:1922–1930
https://doi.org/10.1007/s00261-020-02849-0

HEPATOBILIARY

Modification and comparison of CT criteria in the preoperative assessment of hepatic arterial invasion by hilar cholangiocarcinoma

Qun Zhou[1] · Guoqiang Dong[1] · Qiongjie Zhu[1] · Yudong Qiu[2] · Liang Mao[2] · Jun Chen[3] · Kefeng Zhou[1] · Anning Hu[1] · Jian He[1]

Received: 6 July 2020 / Revised: 23 October 2020 / Accepted: 30 October 2020 / Published online: 7 November 2020

Abstract

Objective To compare the diagnostic performance of three CT criteria and two signs in evaluating hepatic arterial invasion by hilar cholangiocarcinoma.

Methods In this study, we retrospectively reviewed the CT images of 85 patients with hilar cholangiocarcinoma. Modified *Loyer*'s, *Lu*'s, and *Li*'s standards were used to evaluate hepatic arterial invasion by hilar cholangiocarcinoma with the reference of intraoperative findings and/or the postoperative pathological diagnosis. Arterial tortuosity and contact length were also evaluated.

Results *Loyer*'s, *Lu*'s, and *Li*'s standards showed sensitivities of 91.7%, 90.3%, and 72.2%, specificities of 94.0%, 94.5%, and 95.6%, and accuracies of 93.3%, 93.3%, and 89.0%, respectively, in evaluating hepatic arterial invasion by hilar cholangiocarcinoma. *Loyer*'s and *Lu*'s standards and contact length performed better than *Li*'s standard ($P < 0.001$). Arterial tortuosity performed worse than other criteria ($P < 0.001$). The CT criteria performed best in evaluating proper hepatic arterial invasion compared with the left and right hepatic artery. When the cut-off contact length of 6.73 mm was combined with *Loyer*'s standard, 4 false-negative cases could be avoided.

Conclusions *Loyer*'s and *Lu*'s standards and the contact length performed best in evaluating hepatic arterial invasion by hilar cholangiocarcinoma on preoperative CT images, particularly in assessing the proper hepatic artery. Arterial tortuosity could serve as an important supplement. The combination of the contact length and *Loyer*'s standard could improve the diagnostic performance.

Keywords Hilar cholangiocarcinoma · Klatskin tumor · Computed tomography · Hepatic artery · Diagnosis

Abbreviations

ROI	Region of interest
MPR	Multiple planar reconstruction
VR	Volume rendering
MIP	Maximum intensity projection
ROC	Receiver operating characteristic
ICC	Intraclass correlation coefficient
AUC	Area under the ROC curve
ERCP	Endoscopic retrograde cholangio-pancreatography
PTCD	Percutaneous transhepatic cholangial drainage
PVE	Portal vein embolization
CI	Confidence interval

Kefeng Zhou, Anning Hu and Jian He have contributed equally.

Electronic supplementary material The online version of this article (https://doi.org/10.1007/s00261-020-02849-0) contains supplementary material, which is available to authorized users.

✉ Kefeng Zhou
zhoukefeng1977@163.com

✉ Anning Hu
huanning820@sina.com

✉ Jian He
hjxueren@126.com

Extended author information available on the last page of the article

Introduction

Hilar cholangiocarcinoma is a malignant tumor originating from the hilar bile ductal epithelium, with an insidious onset and a dismal prognosis [1]. The tumor accounts for 40–60% of cholangiocarcinoma, with an increasing incidence globally in recent years [2, 3]. To date, surgical

resection remains the only curative treatment for hilar cholangiocarcinoma [4, 5].

Because of its specific anatomic location and infiltrative growth pattern, hilar vascular structures are prone to be invaded by hilar cholangiocarcinoma, which will reduce the resection rate of this complex disease [6]. Therefore, assessing the vascular invasion status is crucial to evaluate resectability, optimize surgical planning, and predict the recurrence and survival of the disease [7–9].

In clinical practice, the most commonly used primary examination for the preoperative evaluation of hilar cholangiocarcinoma remains contrast-enhanced CT. Many studies have used contrast-enhanced CT to investigate vessel invasion. Some have assessed invasion as part of preoperative CT, while others have considered hepatic arterial and portal venous invasion as a whole. Few studies have focused on CT evaluation of the hepatic arterial invasion of hilar cholangiocarcinoma [10, 11]. Previously, we reported that a new diagnostic model of contrast-enhanced CT was useful to assess the portal venous invasion of hilar cholangiocarcinoma. The accurate assessment of hepatic arterial invasion in hilar cholangiocarcinoma is closely related to the R0 resection rate, which is critical for long-term survival. Additionally, some studies have considered that the hepatic arterial invasion of hilar cholangiocarcinoma is a risk factor for tumor recurrence and poor prognosis [7, 8]. Because the hepatic artery is significantly different from the portal vein in terms of vessel elasticity, wall structure, wall thickness, and lumen diameter, the diagnostic criteria for invasion based on CT imaging should be different from each other [12]. However, a lack of dedicated CT criteria exists to assess the invasion of hepatic arteries by hilar cholangiocarcinoma.

We attempted to introduce three CT criteria of pancreatic cancer and modify them exclusively for hilar cholangiocarcinoma because they share some common biological characteristics. *Loyer* et al. [13] and *Lu* et al. [14] proposed CT criteria to assess the resectability of pancreatic cancer based on the relationship between tumors and adjacent vessels, including both arteries and veins. *Li* et al. [12] proposed CT criteria to assess adjacent arterial invasion by pancreatic cancer. Additionally, the diagnostic role of the length of contact between the right hepatic artery and hilar cholangiocarcinoma was indicated by Fukami et al. [15]. Additionally, arterial tortuosity was a common finding on CT images of hilar cholangiocarcinoma, whose diagnostic value has never been reported.

Thus, this study aimed to compare and modify the diagnostic performance of the three CT criteria above and two specific signs in evaluating hepatic arterial invasion by hilar cholangiocarcinoma.

Materials and methods

Patients

This retrospective study was approved by the local ethics committee, and the patient's informed consent was waived. From January 2011 to December 2019, 177 patients were admitted with a clinical diagnosis of hilar cholangiocarcinoma at our hospital. The inclusion criteria for this study were as follows: (1) a pathological diagnosis of hilar cholangiocarcinoma via biliary brushing, biopsy, laparotomy or postoperative specimens; (2) lesions originating from the hilar bile duct rather than intrahepatic or distal cholangiocarcinoma involving the hilar bile duct; (3) definite intraoperative and/or pathological information, indicating that the tumor lesion involved the hepatic arteries; (4) intact preoperative CT imaging data (Fig. 1). Accordingly, 92 cases were excluded, including 52 cases receiving palliative treatment without a pathologic diagnosis due to advanced disease, 13 cases lacking definite intraoperative information of hepatic arterial invasion, and 27 cases with incomplete preoperative CT imaging data. The remaining 85 patients were included in our study cohort, 57 men and 28 women with a mean age of 59 ± 10 years (range 36–81 years).

Of the 85 patients, 76 received surgical resection, and the remaining 9 patients only underwent exploratory laparotomy. Involvement of the hepatic artery by the tumor was confirmed intraoperatively in all the patients, while postoperative pathological assessment was only performed in 4 patients. No patient received neoadjuvant radiotherapy or chemotherapy. Before surgery, 33 patients had undergone endoscopic retrograde cholangiopancreatography (ERCP), 24 received percutaneous transhepatic-cholangial drainage (PTCD), and 7 underwent portal vein embolization (PVE). For those patients, CT imaging after ERCP, PTCD, or PVE and closest to surgery was adopted. The interval between CT imaging and surgery was 11 ± 9 days (range 1–50 days).

CT examination

All the patients underwent CT examination using a multidetector spiral CT scanner (Lightspeed; VCT, or Discovery HD750; GE Healthcare, US) in the supine position. The scan range was from the diaphragm to the pubic symphysis. After plain CT, the patients received a contrast agent of 1.2 mL/kg body weight (Omnipaque 350 mg I/mL; GE Healthcare, US) at a rate of 3.0 mL/s, followed by 40 mL of saline solution through the elbow vein using a power injector (Medrad Stellant, Indianola, PA) at a rate of

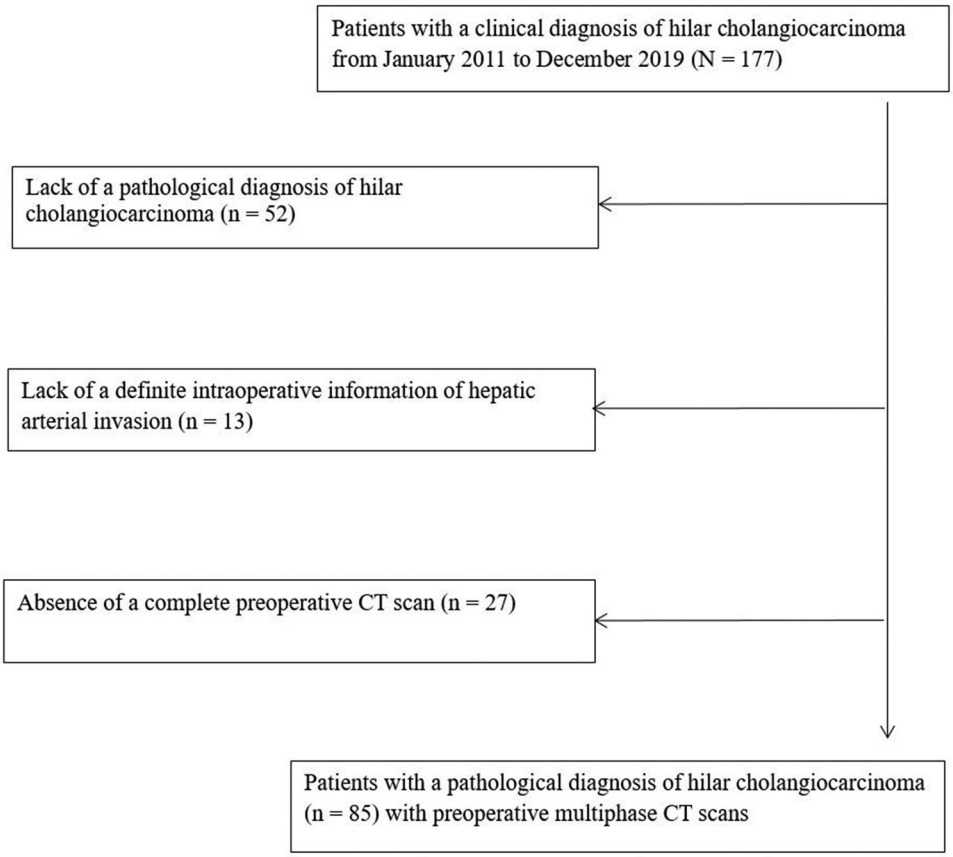

Fig. 1 Inclusion and exclusion flowchart of this study

3.0 mL/s. The early arterial phase was triggered when the CT value of the region of interest (ROI) placed within the aorta at the level of the diaphragm arrived at 150 HU, and the late arterial and portal venous phases were scanned every 20 s after the early arterial phase, each lasting for approximately 7 s. The delayed phase began after 3 min. All the CT images were obtained using a tube voltage of 120 kVp, a tube current of 240–300 mA, a slice interval of 5 mm, a slice thickness of 5 mm, a reconstruction slice of 1.25 mm, a rotation time of 0.6–0.7 s, a helical pitch of 1.375, a matrix of 512 × 512, a field of view of 35–40 cm, and a standard reconstruction algorithm. Multiple planar reconstruction (MPR), maximum intensity projection (MIP) and 3D volume rendering (VR) were performed for image interpretation.

Image analysis

All the CT images were transferred to a workstation (AW4.3; GE Healthcare, US). Two radiologists who were blinded to the clinicopathological information (with 8 and 7 years of experience in abdominal imaging, respectively) independently evaluated hepatic artery involvement according to the following criteria. If there was any contradiction, the two radiologists tried to achieve a consensus through discussion or consulted a senior radiologist (with 13 years of experience in abdominal imaging). The hepatic artery was assessed by three segments, including the proper hepatic artery, left hepatic artery and right hepatic artery. All the evaluations were performed at the arterial phase, with the later arterial phase predominating and early arterial phase supplementing. No recognized diagnostic criteria are available to evaluate hepatic arterial invasion by hilar cholangiocarcinoma, which is close to the pancreas and shares some biological features with pancreatic cancers. In this study, three criteria to assess the vascular invasion of pancreatic cancer were introduced and modified—*Loyer*'s, *Lu*'s and *Li*'s criteria, respectively.

Loyer et al. [13] posed six types according to the relationship between pancreatic cancer and peripancreatic vessels, which were modified to five types dedicated to hilar cholangiocarcinoma in our study: Type A, normal liver tissues and/or fat plane-separated tumor from the adjacent hepatic artery; Type B, the adjacent hepatic artery is inseparable from the hypodense tumor, and the contact point forms a convexity against the vessel; Type C, the adjacent hepatic artery is inseparable from the hypodense tumor, and the contact point forms a concavity against the hepatic artery or partially encircles the vessel; Type D, the adjacent hepatic artery is encircled by the hypodense tumor, and no fat plane is identified between the hepatic

artery and tumor; Type E, the hepatic artery is occluded by the tumor. According to Loyer et al.'s description, types A–B indicated no invasion of the hepatic artery and types C–E indicated invasion of the hepatic artery by hilar cholangiocarcinoma.

Based on the contact angle between the vessel and pancreatic cancer, Lu et al. [14] created 4 grades: grade 0, no contact between the vessels and tumor; grade 1, the contiguity between the tumor and vessel is less than one-quarter of the circumference; grade 2, the contiguity is between one-quarter to one-half of the circumference; grade 3, the contiguity is between one-half to three-quarters of the circumference; grade 4, the contiguity is greater than three-quarters of the circumferential involvement or any hepatic artery constriction. According to Lu et al.'s description, grades 0–2 indicated no invasion of the hepatic artery and grades 3–4 were considered invasion of the hepatic artery by hilar cholangiocarcinoma.

Li et al. [12] proposed that the peripancreatic artery was considered to be invaded with any of the following signs: (a) the tumor occludes the artery; (b) more than one-half circumferential involvement of the arteries by the tumor; (c) the artery wall is irregular; (d) evidence of artery caliber stenosis.

In addition to the above three criteria, two specific signs, hepatic arterial tortuosity and contact length between the artery and tumor, were evaluated. Arterial tortuosity indicates that the hepatic artery becomes markedly tortuous due to pulling by the surrounding tumor tissues (Fig. 2 and Fig. S1). The contact length between the artery and tumor was measured by segments on both axial and coronal CT images, and each segment was summed (Fig. 3). The average value was calculated for statistical analysis [15, 16].

Intraoperative findings and pathological evaluation

Two surgeons (with 25 and 15 years of experience in hepatobiliary surgery, respectively) performed all the surgeries. The involvement status of the hepatic artery by tumors was carefully explored intraoperatively. If the tumor encompassed or occluded the hepatic artery and no blood signals could be detected by intraoperative ultrasonography, the hepatic artery was considered to be involved. The hepatic artery was judged as not involved if it could be separated from the tumor but was surrounded by the tumor. The pathological diagnosis of hepatic arterial invasion based on postoperative specimens was only performed in 4 cases, consistent with the intraoperative findings. The intraoperative findings and/or pathological assessment were deemed the gold standard.

Statistical analyses

Using the intraoperative findings and/or pathological diagnosis as the reference, the diagnostic performance of the above three criteria and two signs in assessing hepatic artery involvement was evaluated by calculating the sensitivity, specificity, accuracy, and positive and negative predictive values. McNemar's test was adopted to compare the diagnostic performance of the criteria and signs. The cut-off value of the contact length was calculated by receiver operating characteristic (ROC) analysis. Interobserver agreement of the three criteria and hepatic arterial tortuosity was evaluated by calculating the kappa value, and the interobserver agreement of the contact length was evaluated using the intraclass correlation coefficient (ICC). Statistical analyses were performed using SPSS 22.0 software (SPSS Inc., Chicago, IL). A P value < 0.05 was considered statistically significant.

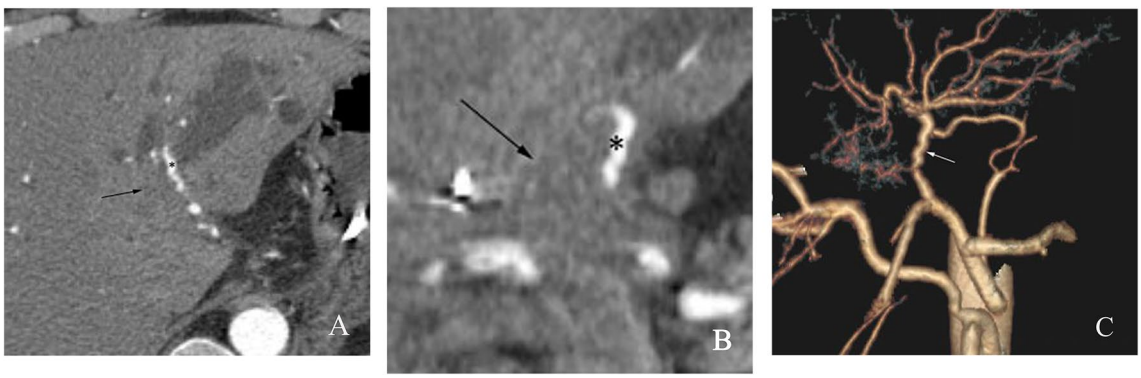

Fig. 2 A 53-year-old male patient with hilar cholangiocarcinoma invading the left hepatic artery, as confirmed by intraoperative findings. **a** Axial CT image in the arterial phase shows the tumor (black arrow) contacts the left hepatic artery (asterisk), which is treated as invaded based on the three CT criteria. **b** The coronal CT image in the arterial phase shows that the tumor (black arrow) wraps the left hepatic artery (asterisk), causing an irregular shape of the arterial wall. **c** The volume-rendering image shows the left hepatic artery as extremely tortuous (white arrow)

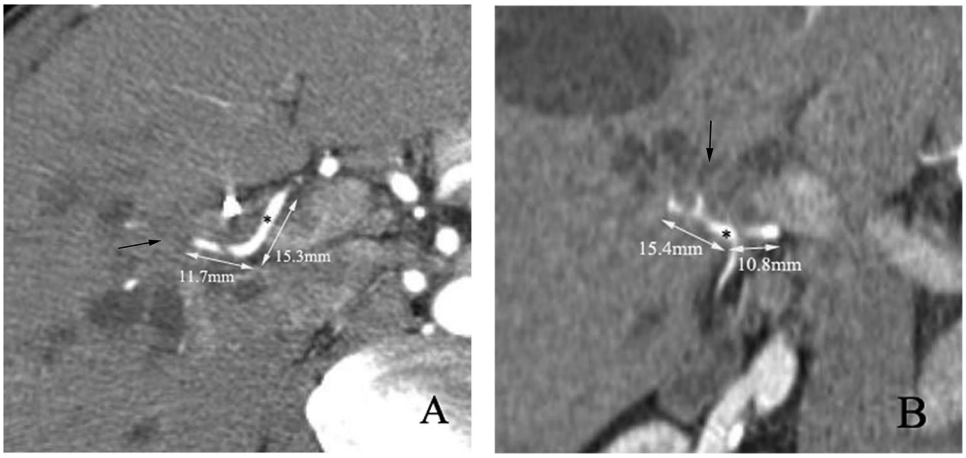

Fig. 3 A 66-year-old male patient with hilar cholangiocarcinoma invading the right hepatic artery, as confirmed by intraoperative findings. **a** The axial CT image in the arterial phase shows that the tumor (black arrow) partially wraps the right hepatic artery (asterisk), and the contact length between tumor and artery is 27.0 mm (the sum of each segment). **b** The coronal CT image in the arterial phase shows that the tumor (black arrow) wraps the right hepatic artery (asterisk) with a contact length of 26.2 mm. The averaged value (26.6 mm) is calculated as the final contact length

Results

Patient characteristic and invasion rate

This study included 85 patients, including 57 men and 28 women with a mean age of 59 years. Among the 85 patients with hilar cholangiocarcinoma, 6 cases had the Bismuth I type, 11 cases had the Bismuth II type, 42 cases had the Bismuth III type and 26 cases had the Bismuth IV type. According to the intraoperative findings and/or pathological diagnosis, the hepatic artery was invaded by the tumor in 52/85 patients (61.2%), with an invasion rate of 12/85 (14.1%) for the proper hepatic artery, 26/85 (30.6%) for the left hepatic artery and 34/85 (40.0%) for the right hepatic artery (Table 1).

Interobserver agreement of CT criteria and signs

Loyer's and *Lu*'s criteria showed excellent interobserver agreement (kappa = 0.949 and 0.948, respectively), while *Li*'s criterion showed good interobserver agreement (kappa = 0.872), in evaluating hepatic arterial invasion by hilar cholangiocarcinoma. The interobserver agreement in evaluating hepatic arterial tortuosity was excellent (kappa = 0.808), and the interobserver agreement in measuring the contact length between the artery and tumor was excellent [ICC = 0.959; 95% confidence interval (CI), 0.945–0.970].

Comparison of the three CT criteria and two signs

According to the ROC analysis in Table 2 and Fig. 4, *Loyer*'s and *Lu*'s standards and the contact length showed the best diagnostic performance (AUC = 0.928, 0.924, and 0.935, respectively), without significant differences among them ($P > 0.528$). *Li*'s standard performed worse

Table 1 Hepatic arterial invasion rate in hilar cholangiocarcinomas with different Bismuth classifications

Bismuth–Corlette classification	PHA	LHA	RHA	HA
Type I	1/6 (16.7%)	0/6 (0%)	1/6 (16.7%)	1/6 (16.7%)
Type II	0/11 (0%)	1/11(9.1%)	3/11(27.3%)	4/11 (36.4%)
Type III	5/42 (11.9%)	15/42(35.7%)	16/42 (38.1%)	28/42 (66.7%)
Type IV	6/26 (23.1%)	10/26 (38.5%)	14/26 (53.8%)	19/26 (73.1%)
Overall	12/85 (14.1%)	26/85 (30.6%)	34/85 (40.0%)	52/85 (61.2%)

The Bismuth classification of each case was confirmed by intraoperative findings

PHA proper hepatic artery, *LHA* left hepatic artery, *RHA* right hepatic artery, *HA* hepatic artery

Table 2 Diagnostic performance of the three CT criteria and two signs

	AUC	SE[a]	95% CI[b]
Loyer's standard	0.928	0.0186	0.889–0.957
Lu's standard	0.924	0.0195	0.884–0.953
Li's standard*	0.839	0.0276	0.788–0.882
Contact Length	0.935	0.0158	0.898–0. 962
Arterial tortuosity[#]	0.679	0.0291	0.618–0.736

*This standard showed a significant difference with that of Loyer's and Lu's standards and the contact length

[#]This sign showed a significant difference with all the other signs and standards

[a]DeLong et al. (1988)

[b]Binomial exact

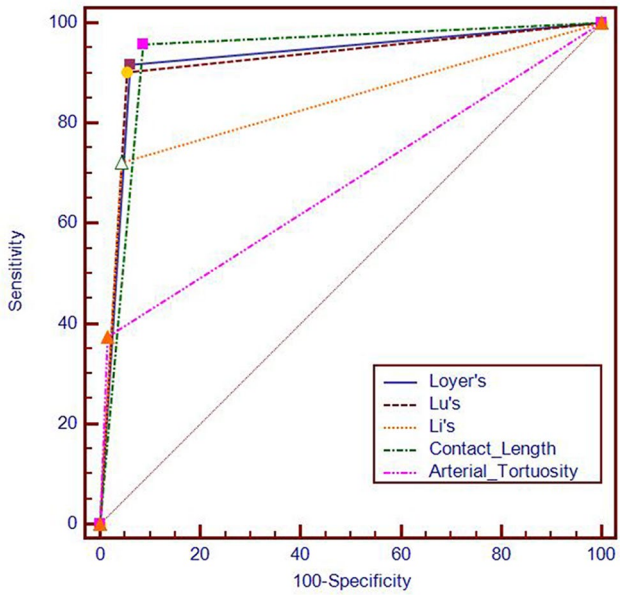

Fig. 4 ROCs of the three standards and two signs

than the above three criteria (AUC = 0.839; $P < 0.001$), while arterial tortuosity performed worst among all the criteria (AUC = 0.679; $P < 0.001$).

To evaluate hepatic arterial segment invasion as a whole ($n = 255$), *Loyer*'s and *Lu*'s standards performed well in the sensitivity, specificity, accuracy, PPV and NPV (85.7–96.6%). *Li*'s standard showed a lower sensitivity (72.2%), but its specificity, accuracy, PPV and NPV were acceptable (86.7–95.6%). For each segment of the hepatic artery, the proper hepatic artery showed the best accuracy at 95.3–98.8%, followed by the left hepatic artery at 92.9–95.3%, and the right hepatic artery at 78.0–85.9% (Table 3).

Table 3 Diagnostic performance of the CT criteria in evaluating hepatic arterial invasion by hilar cholangiocarcinoma, as confirmed by intraoperative findings and/or pathological findings

HA	*Loyer*'s standard					*Lu*'s standard					*Li*'s standard				
	Sensitivity	Specificity	Accuracy	PPV	NPV	Sensitivity	Specificity	Accuracy	PPV	NPV	Sensitivity	Specificity	Accuracy	PPV	NPV
PHA	9/10 (90.0%)	75/75 (100%)	84/85 (98.8%)	9/9 (100%)	75/76 (98.7%)	9/10 (90.0%)	75/75 (100%)	84/85 (98.8%)	9/9 (100%)	75/76 (98.7%)	6/10 (60.0%)	75/75 (100%)	81/85 (95.3%)	6/6 (100%)	75/79 (94.9%)
LHA	25/27 (92.6%)	56/58 (96.6%)	81/85 (95.3%)	25/27 (92.6%)	56/58 (96.6%)	25/27 (92.6%)	56/58 (96.6%)	81/85 (95.3%)	25/27 (92.6%)	56/58 (96.6%)	22/27 (81.5%)	57/58 (98.3%)	79/85 (92.9%)	22/23 (95.7%)	57/62 (91.9%)
RHA	32/35 (91.4%)	41/50 (82.0%)	73/85 (85.9%)	32/41 (78.0%)	41/44 (93.2%)	31/35 (88.6%)	42/50 (84.0%)	73/85 (85.9%)	31/39 (79.5%)	42/46 (91.3%)	24/35 (68.6%)	43/50 (86.0%)	67/85 (78.8%)	24/31 (77.4%)	43/54 (79.6%)
Overall	66/72 (91.7%)	172/183 (94.0%)	238/255 (93.3%)	66/77 (85.7%)	172/178 (96.6%)	65/72 (90.3%)	173/183 (94.5%)	238/255 (93.3%)	65/75 (86.7%)	173/180 (96.1%)	52/72 (72.2%)	175/183 (95.6%)	227/255 (89.0%)	52/60 (86.7%)	175/195 (89.7%)

PHA proper hepatic artery; *LHA* left hepatic artery, *RHA* right hepatic artery, *HA* hepatic artery, *PPV* positive prediction value, *NPV* negative prediction value

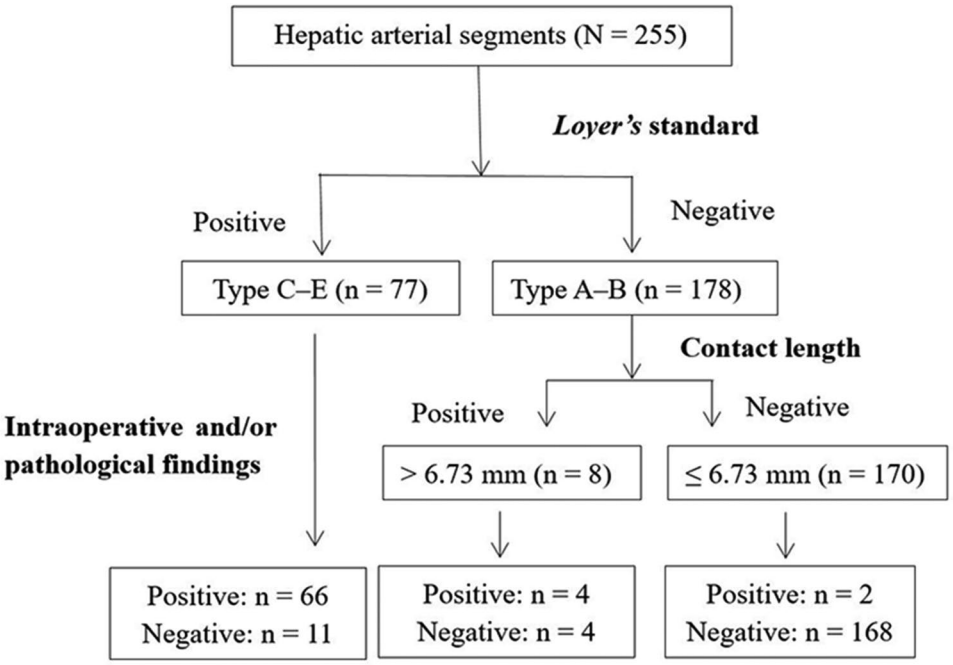

Fig. 5 In total, 255 hepatic arterial segments in 85 patients of hilar cholangiocarcinoma were evaluated in our study. According to *Loyer*'s standard, 77 segments were diagnosed as infiltrated (Type C–E), while 178 segments were noninfiltrated (Type A–B). Among the 178 noninfiltrated segments, 8 segments are treated as infiltrated according to the contact length between the artery and tumor (> 6.73 mm). Finally, 4 of the 8 segments were infiltrated, as confirmed by intraoperative findings

Table 4 Diagnostic performance of hepatic arterial tortuosity in evaluating hepatic arterial invasion by hilar cholangiocarcinoma, as confirmed by intraoperative findings and/or pathological findings

Hepatic artery	Sensitivity	Specificity	Accuracy	PPV	NPV
PHA	1/10 (10.0%)	75/75 (100%)	76/85 (89.4%)	1/1 (100%)	75/84 (89.2%)
LHA	13/27 (48.1%)	58/58 (100%)	71/85 (83.5%)	13/13 (100%)	58/72 (80.6%)
RHA	13/35 (37.1%)	47/50 (94.0%)	60/85 (70.6%)	13/16 (81.2%)	47/69 (68.1%)
Overall	27/72 (37.5%)	180/183 (98.4%)	207/255 (81.2%)	27/36 (90.0%)	180/225 (80.0%)

PHA proper hepatic artery, *LHA* left hepatic artery, *RHA* right hepatic artery, *HA* hepatic artery, *PPV* positive prediction value, *NPV* negative prediction value

With the cut-off of 3.60 mm, the contact length between the artery and tumor showed an accuracy of 92.5%, a specificity of 91.2%, a sensitivity of 95.8%, a PPV of 81.2% and an NPV of 98.2% in evaluating the invasion of the hepatic artery by hilar cholangiocarcinoma. By combining the contact length and *Loyer*'s standard, 4 of 8 false-negative cases could be avoided, resulting in a sensitivity of 97.2%, a specificity of 91.8%, an accuracy of 93.3%, a PPV of 82.4%, and an NPV of 98.8% (Fig. 5).

Hepatic arterial tortuosity showed a low sensitivity of 37.5% but a high specificity of 98.4% (Table 4). Based on segmental evaluation, this sign performed well in evaluating proper and left hepatic arterial invasion, but poorly in evaluating right hepatic arterial invasion.

Discussion

This study included 85 patients with hilar cholangiocarcinoma and a hepatic arterial invasion rate of 61.2%. There were 17 cases of Bismuth types I–II (20.0%) and 68 cases of types III–V (80.0%), findings that agreed with other study findings [17, 18]. The hepatic arterial invasion rate was 29.4% in Bismuth types I–II and 69.1% in types III–IV, findings that were also consistent with previous findings [9, 19, 20].

We found that *Loyer*'s and *Lu*'s standards performed well with excellent interobserver agreement, while *Li*'s standard performed relatively poorly in evaluating hepatic

arterial invasion by hilar cholangiocarcinoma. *Loyer*'s and *Lu*'s standards are based on the relationship and contact angle between the hepatic artery and tumor qualitatively and quantitatively, respectively [13, 14]. *Li*'s criterion is based on only several specific signs, which are easily affected by the observer's experience and appear less systematic [12].

However, the CT criteria were associated with false-positive and false-negative findings. For example, in our study, 10 cases were judged as type C in *Loyer*'s standard and grade 3 in *Lu*'s standard but were positive findings on CT imaging. However, those hepatic arteries could be removed during surgery and the Glisson sheath surrounding the hepatic artery was infiltrated by hilar cholangiocarcinoma, which caused diagnostic pitfalls on CT imaging [12]. Another 6 cases were judged as type A in *Loyer*'s standard and grade 1 in *Lu*'s standard but were negative findings on CT imaging. However, those arteries were found to be infiltrated by the tumor, as confirmed with intraoperative findings.

Therefore, besides the three criteria, we also focused on two specific CT signs, arterial tortuosity and the contact length between the tumor and hepatic artery. Arterial tortuosity due to the tumor's infiltration into the arterial wall [12, 21] could reduce false positivity because of its high specificity and positive predictive value in evaluating hepatic arterial invasion. The CT criteria neglected the contact length between the tumor and hepatic artery, while the contact length is critical to assess the resectability of hilar cholangiocarcinoma [15, 16]. It is difficult to strip the tumor from the hepatic artery if the contact length reaches a certain level. The contact length showed an excellent performance in evaluating hepatic arterial invasion with an AUC of 0.935, which could serve as an essential index in evaluating hepatic arterial invasion. Fukami et al. [15] reported that, with a cut-off value of 10.9 mm, the contact length showed an accuracy of 77.4%, a sensitivity of 76.3% and a specificity of 80.0% in evaluating right hepatic arterial invasion by hilar cholangiocarcinoma.

Subsequently, we combined *Loyer*'s standard and the contact length to evaluate hepatic arterial invasion. If *Loyer*'s standard showed a negative finding, but the contact length was > 6.73 mm, the hepatic artery was still treated as being invaded by the tumor. Thus, a sensitivity of 97.2% and a specificity of 91.8% were achieved.

Additionally, we found that the invasion rate and diagnostic performance of the CT criteria were different in each segment of the hepatic artery in patients with hilar cholangiocarcinoma. The invasion rate of the proper hepatic artery (14.1%) was lower than that of the left (30.6%) and right hepatic arteries (40.0%). The CT criteria performed best in evaluating invasion of the proper hepatic artery, followed by the left and right hepatic arteries, probably due to the following three reasons. First, the proper hepatic artery appears straight, making it easily observed on serial axial CT images. Second, the left hepatic artery has a thin lumen, which can easily be wrapped by the tumor [22]. Third, the right hepatic artery runs behind the common hepatic duct with a relatively long distance outside the liver parenchyma, whose Glisson sheath is easily invaded by hilar cholangiocarcinoma, possibly causing false-positive findings [12, 21, 23–25].

This study possessed limitations. First, the sample size was not sufficiently large but larger than multiple previous studies [15, 25, 26]. Second, the study was retrospective in design and most patients lacked postoperative pathologic information. Third, we did not evaluate the invasion depth of the hepatic artery by the tumor, a feature that is also important to guide surgery [9, 15, 16, 27]. We will perform a prospective study to address those issues in the future.

In conclusion, *Loyer*'s and *Lu*'s standards performed best in evaluating hepatic arterial invasion by hilar cholangiocarcinoma with good interobserver agreement. Their diagnostic performance in evaluating the proper and left hepatic arteries was better than that for the right hepatic artery. The combination of the contact length and *Loyer*'s standard could improve the diagnostic performance.

Acknowledgements The authors thank the hepatobiliary pancreatic tumor multidisciplinary team in Nanjing Drum Tower Hospital

Funding No funding.

Compliance with ethical standards

Conflict of interest All authors declare that they have no conflict of interest.

References

1. Cai WK, Lin JJ, He GH, Wang H, Lu JH, Yang GS. Preoperative serum CA19-9 levels is an independent prognostic factor in patients with resected hilar cholangiocarcinoma. Int J Clin Exp Pathol 2014; 7:7890-7898.
2. Abd ElWahab M, El Nakeeb A, Hanafy EE, et al. Predictors of long term survival after hepatic resection for hilar cholangiocarcinoma: A retrospective study of 5-year survivors. World Journal of Gastrointestinal Surgery 2016; 8:436.
3. Furusawa N, Kobayashi A, Yokoyama T, Shimizu A, Motoyama H, Miyagawa S. Surgical Treatment of 144 Cases of Hilar Cholangiocarcinoma Without Liver-Related Mortality. World J Surg 2014; 38:1164-1176.
4. Dinant S, Gerhards MF, Rauws EAJ, Busch ORC, Gouma DJ, van Gulik TM. Improved Outcome of Resection of Hilar Cholangiocarcinoma [Klatskin Tumor]. Ann Surg Oncol 2006; 13:872-880.
5. Nagino M, Ebata T, Yokoyama Y, et al. Evolution of Surgical Treatment for Perihilar Cholangiocarcinoma. Ann Surg 2013; 258:129-140.
6. Ito F, Cho CS, Rikkers LF, Weber SM. Hilar Cholangiocarcinoma: Current Management. Ann Surg 2009; 250:210-218.

7. Hu H. Prognostic factors and long-term outcomes of hilar cholangiocarcinoma: A single-institution experience in China. World J Gastroentero 2016; 22:2601.
8. Wang ST, Shen SL, Peng BG, et al. Combined vascular resection and analysis of prognostic factors for hilar cholangiocarcinoma. Hepatobiliary Pancreat Dis Int 2015; 14:626-632.
9. Matsuyama R, Mori R, Ota Y, et al. Significance of Vascular Resection and Reconstruction in Surgery for Hilar Cholangiocarcinoma: With Special Reference to Hepatic Arterial Resection and Reconstruction. Ann Surg Oncol 2016; 23:475-484.
10. Oshiro Y, Sasaki R, Nasu K, Ohkohchi N. A novel preoperative fusion analysis using three-dimensional MDCT combined with three-dimensional MRI for patients with hilar cholangiocarcinoma. Clin Imag 2013; 37:772-774.
11. Nagakawa Y, Kasuya K, Bunso K, et al. Usefulness of multi-3-dimensional computed tomograms fused with multiplanar reconstruction images and peroral cholangioscopy findings in hilar cholangiocarcinoma. J Hepato-Bil-Pan Sci 2014; 21:256-262.
12. Li H, Zeng MS, Zhou KR, Jin DY, Lou WH. Pancreatic adenocarcinoma: the different CT criteria for peripancreatic major arterial and venous invasion. J Comput Assist Tomogr 2005; 29:170-175.
13. Loyer EM, David CL, Dubrow RA, Evans DB, Charnsangavej C. Vascular involvement in pancreatic adenocarcinoma: reassessment by thin-section CT. Abdom Imaging 1996; 21:202-206.
14. Lu DS, Reber HA, Krasny RM, Kadell BM, Sayre J. Local staging of pancreatic cancer: criteria for unresectability of major vessels as revealed by pancreatic-phase, thin-section helical CT. AJR Am J Roentgenol 1997; 168:1439-1443.
15. Fukami Y, Ebata T, Yokoyama Y, et al. Diagnostic ability of MDCT to assess right hepatic artery invasion by perihilar cholangiocarcinoma with left-sided predominance. J Hepato-Bil-Pan Sci 2012; 19:179-186.
16. Furukawa H, Iwata R, Moriyama N. Angiographic assessment of the right hepatic artery for encasement by hilar cholangiocarcinoma: Comparison between antero-posterior and right anterior oblique projections. Cardiovasc Inter Rad 2001; 24:37-41.
17. Ismael HN, Loyer E, Kaur H, Conrad C, Vauthey JN, Aloia T. Evaluating the Clinical Applicability of the European Staging System for Perihilar Cholangiocarcinoma. J Gastrointest Surg 2016; 20:741-747.
18. Valls C, Ruiz S, Martinez L, Leiva D. Radiological diagnosis and staging of hilar cholangiocarcinoma. World J Gastrointest Oncol 2013; 5:115-126.
19. Tan JW, Hu BS, Chu YJ, et al. One-stage resection for Bismuth type IV hilar cholangiocarcinoma with high hilar resection and parenchyma-preserving strategies: a cohort study. World J Surg 2013; 37:614-621.
20. Govil S, Reddy MS, Rela M. Surgical resection techniques for locally advanced hilar cholangiocarcinoma. Langenbecks Arch Surg 2014; 399:707-716.
21. Kawarada Y, Das BC, Taoka H. Anatomy of the hepatic hilar area: the plate system. J Hepatobiliary Pancreat Surg 2000; 7:580-586.
22. Nakanishi Y, Zen Y, Kawakami H, et al. Extrahepatic bile duct carcinoma with extensive intraepithelial spread: a clinicopathological study of 21 cases. Mod Pathol 2008; 21:807-816.
23. Senda Y, Nishio H, Oda K, et al. Value of Multidetector Row CT in the Assessment of Longitudinal Extension of Cholangiocarcinoma—Correlation Between MDCT and Microscopic Findings. World J Surg 2009; 33:1459-1467.
24. Ebata T, Nagino M, Kamiya J, Uesaka K, Nagasaka T, Nimura Y. Hepatectomy With Portal Vein Resection for Hilar Cholangiocarcinoma. Ann Surg 2003; 238:720-727.
25. Burke EC, Jarnagin WR, Hochwald SN, Pisters PW, Fong Y, Blumgart LH. Hilar Cholangiocarcinoma: patterns of spread, the importance of hepatic resection for curative operation, and a presurgical clinical staging system. Ann Surg 1998; 228:385-394.
26. Endo I, Shimada H, Sugita M, et al. Role of three-dimensional imaging in operative planning for hilar cholangiocarcinoma. Surgery 2007; 142:666-675.
27. Okumoto T, Sato A, Yamada T, et al. Correct diagnosis of vascular encasement and longitudinal extension of hilar cholangiocarcinoma by four-channel multidetector-row computed tomography. Tohoku J Exp Med 2009; 217:1-8.

Affiliations

Qun Zhou[1] · Guoqiang Dong[1] · Qiongjie Zhu[1] · Yudong Qiu[2] · Liang Mao[2] · Jun Chen[3] · Kefeng Zhou[1] · Anning Hu[1] · Jian He[1]

[1] Department of Radiology, Nanjing Drum Tower Hospital, The Affiliated Hospital of Nanjing University Medical School, No. 321 Zhongshan Road, Nanjing 210008, Jiangsu Province, China

[2] Department of Hepatopancreatobiliary Surgery, Nanjing Drum Tower Hospital, The Affiliated Hospital of Nanjing University Medical School, No. 321 Zhongshan Road, Nanjing 210008, Jiangsu Province, China

[3] Department of Pathology, Nanjing Drum Tower Hospital, The Affiliated Hospital of Nanjing University Medical School, No. 321 Zhongshan Road, Nanjing 210008, Jiangsu Province, China